The chemical elemental demixing in the simulation of air and CO_2 plasma flows in the inductive plasmatron chamber

V.I. Sakharov and D.Yu. Khanukaeva***
**Institute of Mechanics Moscow State University*
1 Michurinskii Prospect, 119192 Moscow, Russia, Email: sakharov@imec.msu.ru
***Gubkin Russian State University of Oil and Gas*
65 Leninskii Prospect, 119991, Moscow, Russia, Email: khanuk@yandex.ru

Abstract

The gas plasma flows in the plasmatron torch with a sonic nozzle were numerically simulated in the frame of the Navier-Stokes equations for the test conditions of the 100-kW IPG-4 facility of the Institute for Problems in Mechanics, Russian Academy of Sciences (IPM RAS). The regions of chemical elemental demixing in the flow were discovered in the examination of the obtained solutions. The origination of these regions along with their possible influence on the heat transfer to the bodies in the underexpanded flows in physical experiments is explained.

1. Introduction

The effect of diffusive chemical elemental demixing due to differences in diffusive properties of chemical components was first discovered and studied in the analysis of air mixture flow in a multicomponent boundary layer near the stagnation point on a catalytic wall [1-4]. In [1, 3] the Stephan-Maxwell relations [5] were used as the diffusion model. Conclusions were made both for a frozen boundary layer, and at finite rates of chemical reactions within it. In [2] the Fick laws with the effective diffusion coefficients for the groups of components were taken as the diffusion model; the influence of the atomic composition on the outer edge of the frozen boundary layer on the demixing effect was studied. In [4] it was shown, that chemical elemental demixing is absent if it is used one and the same coefficient of binary diffusion of an atomic-molecular mixture for all mixture components. It was noted, that thermal diffusion contributes lightly into elemental demixing, and has almost no effect on heat transfer and friction.
The chemical elemental demixing was also obtained in the rigorous numerical computation of the five-components air mixture flow in a chemically nonequilibrium boundary layer in the vicinity of a blunt body stagnation point [6].
In [7] the solution for a multicomponent chemically nonequilibrium boundary layer near catalytic wall in the vicinity of the stagnation point was asymptotically investigated. The elemental demixing was obtained to be effectively dependent on the atomic concentration at the outer edge of the boundary layer and the character of homogeneous and heterogeneous chemical reactions proceeding. On the basis of the obtained asymptotic formulas for the five-components air boundary layer it was concluded that regions with higher (or lower) values of oxygen or nitrogen concentrations are formed on the body surface depending on its catalytic properties with respect to nitrogen and oxygen atoms recombination. Also it was demonstrated, that chemical elemental demixing may take place likewise on a non-catalytic wall due to the difference in the recombination rates for various atomic components of the gaseous phase.
The effect of chemical elemental demixing was also observed in chemically equilibrium flows [8]. It was noted, that such flows description must include both diffusion equations for the reactions products, and the diffusion equations for all elements of the mixture instead of the conditions of element composition conservation. The main reason of the demixing effect in this case is also the difference of diffusion coefficients for various mixture components.
The results of simulation of air plasma flows in the Von Karman Institute (VKI), Brussels, Belgium Plasmatron torch and exhaust sonic jet are given in [9,10]. The elemental demixing effect was obtained both for chemically equilibrium and non equilibrium flows. Owing to the constructive features of the VKI facility, the elemental demixing in it occurs presumably in the radial direction due to large gradients of the temperature and the elements concentrations in this direction.
Numerical simulation of flows in the plasmatron torch of IPG-4 facility (IPM RAS) and multi-parametric calculations of heat transfer to the body surfaces from the gas flows has become possible owing to the development

of new numerical methods and modern computational technologies for modelling of plasmas and viscous high-temperature gaseous flows [11-16].
The calculation techniques for subsonic flows of equilibrium plasma of air and other gases in the plasmatron torch and exhaust subsonic jets were developed in IPM RAS [11, 12].
The technology for calculation of sub- and supersonic chemically nonequilibrium flows, based on the software package including programs for numerical integration of the Navier-Stokes equations [13] and special programs-generators interacting with databases of thermodynamic and transfer properties of individual gases [17], is used for the simulation of the flows in the plasmatron torch with sonic nozzles and in the exhaust jets. Such flows and heat transfer to the cylindrical bodies in under-expanded jets of air plasma for various gas models were studied and compared with experimental data in [15, 16].

2. The calculation of the induction plasma flow in the tourch of the IPG-4 plasmatron with a sonic nozzle

In the present work the numerical simulation of ICP air and CO_2 flows was fulfilled for the 100 kW IPG-4 (IPM RAS) test conditions The torch geometry is shown in Fig.1. The torch represents the quartz cylindrical tube of L = 400 mm in length and D_c = 80 mm in diameter. An annular nozzle is located in the lower part of the channel; conical sonic nozzle of the cutoff diameter of D_s is located in the upper part of the channel. The gas of temperature $T\infty$ with permanent flow rate G is supplied through the annular nozzle with the swirl of 45° with respect to its axis, and then the gas is heated by the high frequency electric field and flows out through the conical nozzle into the low-pressure chamber with gas pressure P_∞ and temperature T_∞.

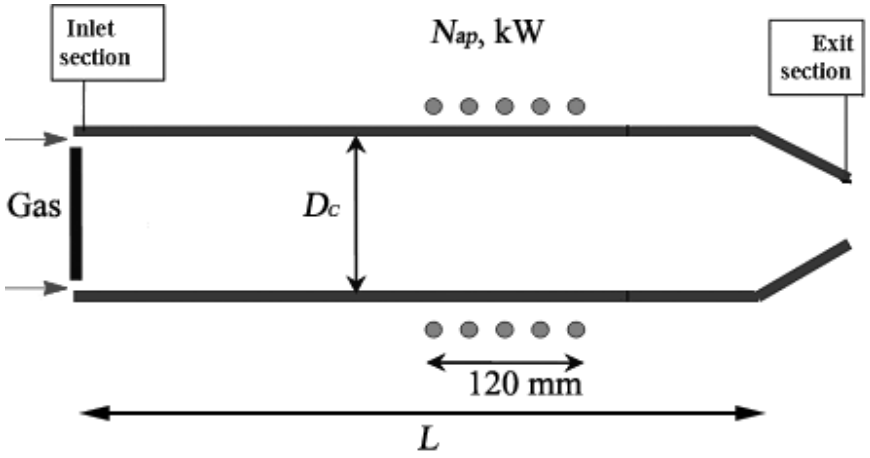

Figure 1: IPG-4 plasmatron torch geometry

The real inductor was replaced by five infinitely thin current loops in the calculations. The high-frequency vortical electric field was modelled in the one-dimensional approach of Maxwell equations using the following assumptions: the electromagnetic field is monochromatic with a given frequency, defined by the high-frequency current in the inductor (the current frequency in the inductor is 1.76 MHz); the plasma is quasi-neutral; the magnetic permeability of the plasma $\mu = 1$; the dielectric permeability of the plasma is independent of the electromagnetic field and, consequently, of the coordinates; the displacement current can be neglected; the variation of the electric field in the axis direction is negligible in comparison with its variation in the radial direction. The complete formulation of the electric part of the problem is given in [12].
The gas flow in the torch was modelled by the system of time-dependent Navier-Stokes equations in the quasi 3-dimensional formulation. The finite volume method (FVM) on the structured curvilinear mesh was used for the numerical solution of the system. The system of FVM finite-difference equations included numerical equivalents of the conservation laws for the quadrangular cells, covering the computation domain, and the difference approximations of the boundary conditions. The values of physical variables – pressure, temperature, velocity vector, species concentrations – were approximately defined by the finite volume method in the centre of each cell and on the middles of each side for the cells, lying on the wall. The inviscid numerical fluxes through the cells sides were defined according to the solution of the Riemann problem of arbitrary discontinuity breakdown [18]. The values of viscous fluxes through the cells sides were calculated using central and one-sided second order difference formulas.

The difference equations were solved with the aid of a two-layer implicit iteration scheme, based on the implicit approximation of the time-dependent Navier-Stokes equations. The splitting of the numerical fluxes Jacobians taking into account the signs of their eigen values was used in the implicit iteration operator construction. The approximate inversion of the implicit operator was realised using the Gauss-Seidel line space-marching method with LU-decomposition in the block-tridiagonal matrices to find solution in every line step.
The following boundary conditions were used: all the necessary parameters of the flow together with the swirl were assigned in the entry section. The symmetry conditions were used at the torch axis. The "non-reflecting" boundary conditions were assigned in the exit section of the computation domain, since the flow over the cylindrical model placed in the low-pressure chamber of the plasmatron was calculated simultaneously. The zero velocity vector and certain temperature values were taken for all the rigid surfaces (the wall of the quartz tube, the endface of the entry section of the chamber, the sonic nozzle and the cylindrical body surfaces). The torch wall was assumed to be noncatalytic with respect to the recombination of the atomic components of the dissociated and partially ionised mixture. The complete problem formulation is given in [15, 16].
Calorimetric measures of the output power of the torch [12] were used in order to define the power supplied to the discharge, N_{pl}. The latter, in turn, was used as the defining parameter in the joined computations of the air mixture flow and the electromagnetic field in the plasmatron torch, the corresponding current in the inductor being found in the solution process.

2.1 Thermochemical and transport models

In the present work the gases were considered as an ideal mixture of perfect gases, where chemical reactions and ionisation reactions may proceed. Rotational and vibrational energy modes of molecules were described by the "rigid rotator-harmonic oscillator" model with the Boltzmann distribution of the energy levels. All of the components were assumed to be in the ground electronic state, and rotational temperature of molecules is equal to their translational temperature. During the computations the air is considered as a mixture of 11 neutral and ionised components: O, N, O_2, NO, N_2, O^+, N^+, NO^+, O_2^+, N_2^+ and e^- and CO_2 is considered as a mixture of: O, C, O_2, CO, CO_2, O^+, C^+, CO^+, O_2^+, C_2 and e^-. The thermodynamic and thermochemical data for the components considered were taken from [17]. The numerical values of the constants for chemical reaction proceeding in the high-temperature air mixture were taken from [19-26].
Special attention must be given to the transport properties for the computation of viscous fluxes of the components masses, the momentum and the energy in the gas. The molar diffusion fluxes were determined from the Stefan-Maxwell relations [5]. Barodiffusion and thermal diffusion were neglected. The viscosity and thermal conductivity coefficients of the gas mixture were calculated by approximate Wilkie-Vasiliyeva formulas [27]. The plasma conductivity was determined from the Stefan-Maxwell relation for the electron component neglecting the heavy particles diffusion and the parameters gradients in the azimuthal direction [16].
The binary diffusion coefficients were calculated using the two-parametric interpolation formula [28] via the cross sections of diffusive type elastic collisions of neutral atoms and molecules with each other and with ions. The formula mentioned is based on the values of the collision cross-sections at low temperature (T_1 = 300 K) and high temperature (T_2 = 20 000 K). The interaction of charged particles is described in the pairwise collisions approximation using the shielded Coulomb potential. The collision integrals for this type of interaction are calculated using approximation dependences, given in [29]. The ratio of all the collision cross-sections of "viscous" type to the corresponding cross-sections of "diffusive" type was assumed for all the components to be equal to 1.1 in the determination of the Schmidt numbers, necessary for the calculation of the viscosity and thermal conductivity coefficients.

3. The results of the computations for air flow

The computations were fulfilled for two regimes of the air mixture flow in the plasmatron torch: G = 2.4 g/s, N_{pl} = 29 kW, D_s = 40 mm (regime I) and G = 4.8 g/s, N_{pl} = 41 kW, D_s = 30 mm (regime II). The second regime differs from the first one in the higher value of flow rate, supplied to the chamber, G; and higher value of the power supplied to the discharge, N_{pl}; the diameter of the nozzle exit section D_s being smaller. The second regime gives rise to the flow in the torch with a lower longitudinal velocity and higher pressure, which is almost constant over the whole torch except for a region adjacent to the sonic nozzle.
The shadowgraph of the isotherms in the plasmatron torch is presented in Fig.2, the vertical dimension being doubled. White curves represent the streamlines. Due to the difference in the intensity of the inductive gas heating the temperature in the torch reaches the value of 13 000 K for regime II contra the value of 11 900 K for regime I. The temperatures at the exit section of the torch also differ. Fig.2 demonstrates a complicated flow pattern formed in the torch with two embedded in one another reverse circulation zones, forming ahead of the inductor. Points S_1 and

S_2 in Fig.2 correspond to the stagnation points of the flow on the symmetry axis. These zones formation is typical for all regimes of the IPG-4 plasmatron operation, both subsonic [11, 12] and supersonic regime with sonic nozzles [15]. The shape and the dimension of the circulation zones are also dependent on the values of operation parameters and the sonic nozzle exit diameter. The comparison of the flow patterns, shown in Fig.2, demonstrates that the increase in the flow rate of the injected gas and the power applied to the plasma and the decrease in the nozzle exit diameter lead to the shortening of the circulation zones and modification of their shape. Thus, the length of the internal circulation zone along the *X*-axis in regime II is half as large as that in regime I.

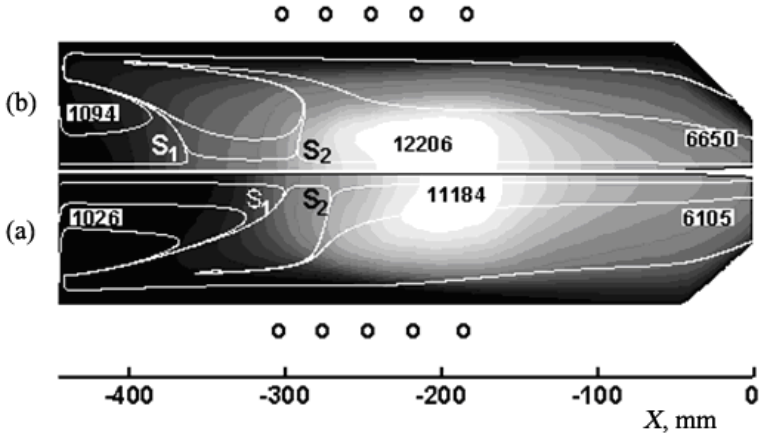

Figure 2: Isotherms and streamlines in the plasmatron torch for regimes I (a) and II (b)

The gas flow in the vicinity of the symmetry line of the plasmatron torch within the first circulation zone with the stagnation point S_1 is qualitatively similar to a flow in the stagnation point region on a blunt body. The difference consists in the following. The recombination of atoms occurs in the boundary layer near the wall with low temperature. Quite the contrary, further dissociation of molecules takes place in the plasmatron due to the temperature rise in the inductor zone, besides the diffusion is possible in any direction from the stagnation point S_1. In the vicinity of the stagnation point S_1 the oxygen dissociation occurs, while the molecular nitrogen concentration remains constant. Oxygen atoms, as being more mobile, diffuse from the region of the stagnation point S_1 more intensively than molecular components arrive there. This leads to oxygen "depletion" of the flow (minimum value $C_o^* = 0.182$). The mass concentration of any chemical element is given by the formula

$$C_l^* = \sum_{j=1}^{N} \frac{n_{jl} m_l C_j}{m_j}, \qquad l = 1, \ldots, L. \qquad \textbf{(1)}$$

Here, n_{jl} is the amount of chemical elements with number l in component j, m_l is the mass of the l-th element, C_j and m_j are the mass concentration and the mass of the j-th component, N is the number of mixture components, L is the number of chemical elements.

So, chemical elemental demixing takes place. The oxygen concentration decreases, while the nitrogen concentration increases. The reason of this demixing connected with the difference in the rates of the dissociation reactions for oxygen and nitrogen molecules. On the contrary, the demixing effect in the region of stagnation point on a blunt body in a supersonic flow leads to the growth of the oxygen element concentration and the diminishing of the nitrogen element concentration [1-3, 6-8].

The confirmation of this explanation one can see from Fig.3. It represents the distributions of the non-charged components of the dissociated air flow and those of oxygen and nitrogen elements along the symmetry axis of the flow. Up to the stagnation point S_1 the mass concentration of the atomic oxygen increases, while that of the molecular oxygen decreases, the concentration of molecular nitrogen remaining constant. Intensive diffusion of the atomic oxygen from this region leads to the decrease of the oxygen element and increase of nitrogen one. Intensive start of the nitrogen molecules dissociation begins in the second circular zone and downstream, in the vicinity of the symmetry axis of the torch, oxygen having been completely dissociated. Atomic nitrogen diffuses from this zone more rapidly than molecular components diffuse in it. Therefore the concentration of the nitrogen element decreases, whereas the oxygen element concentration increases.

Fig. 4 represents the vector field of oxygen element diffusion fluxes in the torch on the background of the concentration shadowgraph of this element for regimes I and II. One can see the demixing effect leading to the diminishing of the oxygen concentration near the symmetry axis of the torch ($X \approx$ -300 mm) in the first reverse-circulation zone. Fig. 4 also shows some other zones with the demixing effect due to the difference in the recombination rates of atomic components and in the values of the diffusion coefficients for atoms and molecules of the gas mixture. The oxygen diffusion toward the symmetry axis and the wall of the torch takes place from the toroidal-shaped region at the point of its connection with the sonic nozzle, which leads to a decrease in the oxygen element concentration in this zone. The oxygen element accumulates near the symmetry axis and near the wall of the torch, its concentration rises up to the value of $C_O^* = 0.255$ near the wall. The accumulation of the oxygen element in the vicinity of the symmetry axis of the torch means that the flow over the body placed in the low-pressure chamber possesses higher concentration of this element, which may intensify the oxidation of the body surface.

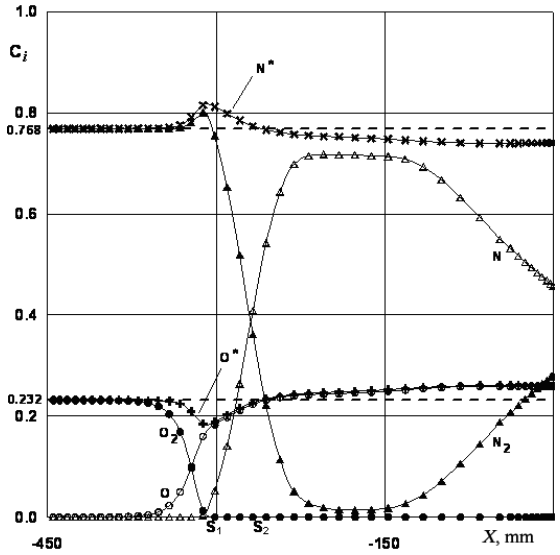

Figure 3: Distributions of the concentrations of components and chemical elements of the air mixture along the flow symmetry axis for regime I

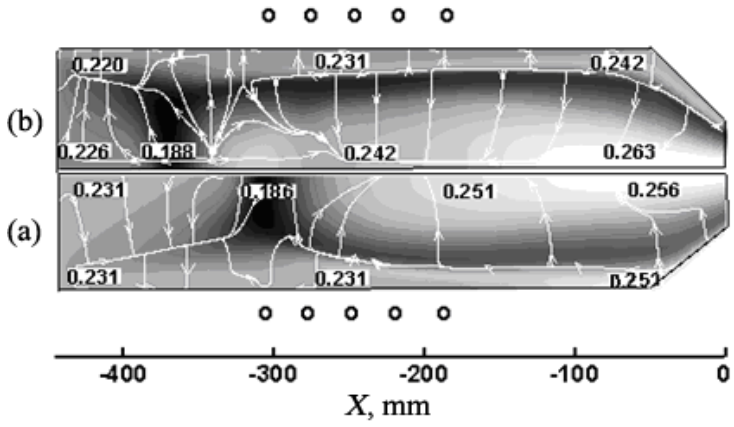

Figure 4: Shadowgraphs of the oxygen element concentration and vector field of its diffusive fluxes in the plasmatron torch for regimes I (a) and II (b)

In Fig.5 the regions of chemical elemental demixing and oxygen element concentration along the symmetry axis of the torch are compared for two regimes considered. The regions of the chemical elemental demixing are shifted toward the endface of the torch along its symmetry axis for the regime II in comparison with the regime I (Fig.5). This correlates with the displacement of the embedded separation zones in the same direction for these cases (Fig. 2). Fig. 6 demonstrates the distribution of the same parameters as in Fig. 3 for regime I in the radial direction for two values of the coordinate $X \approx$ -300 mm (a) and $X \approx$ -100 mm (b). The first section is located close to the stagnation

point S_1. The nitrogen element concentration increases in this zone (Fig. 3), while the chemical elemental demixing is not yet observable near the wall of the torch, since the cold air supplied to the plasmatron torch through the annular nozzle flows chiefly along its wall (R = 40 mm). An increase in the oxygen element concentration near the wall at $X \approx$ -100 mm occurs due to the atomic oxygen recombination.

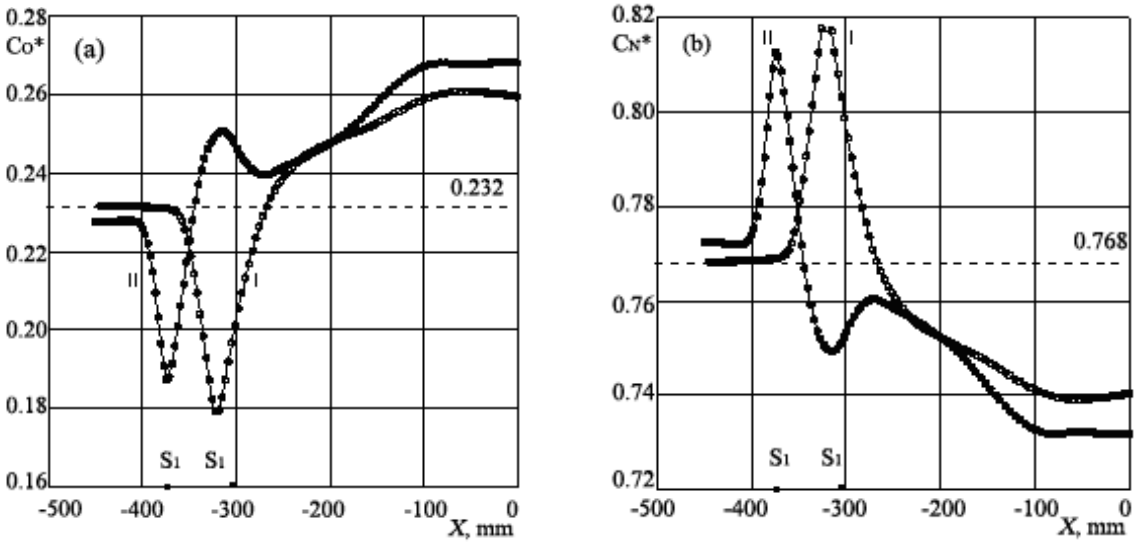

Figure 5: Distribution of the oxygen (a) and nitrogen (b) element concentrations along the symmetry axis of the torch for regimes I and II

The latter, in turn, arrives there owing to its diffusion from the toroidal region, the diffusion of molecular components in the reverse direction being slower. Since the torch wall was assumed to be non-catalytic, the chemical elemental demixing near it is also explained by oxygen atoms recombination in absence of atomic nitrogen and the difference in the diffusion rates for the atomic and molecular components of the mixture.

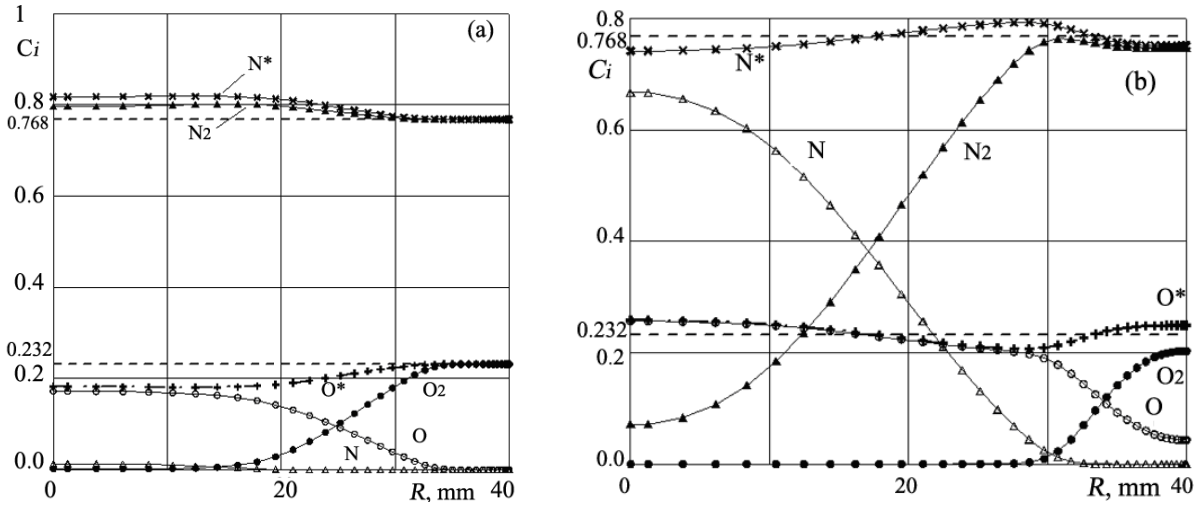

Figure 6: Distribution of the concentrations of components and chemical elements of the air mixture in the radial direction for regime I at X = –300 mm (a) and X = –100 mm (b)

3. The results of the computations for CO_2 flow

The computations were fulfilled for two regimes of the CO_2 mixture flow in the plasmatron torch: G = 2.4 g/s, N_{pl} = 23 kW, D_s = 30 mm (regime I) and G = 4.8 g/s, N_{pl} = 32 kW, D_s = 30 mm (regime II). The second regime differs from the first one in the higher value of flow rate, supplied to the chamber, G; and higher value of the power

supplied to the discharge, N_{pl}. The second regime gives rise to the flow in the torch with a lower longitudinal velocity and higher pressure, which is almost constant over the whole torch except for a region adjacent to the sonic nozzle.
In Fig.7(a) the regions of chemical elemental demixing and oxygen element concentration along the symmetry axis of the torch are compared for two regimes considered. The regions of the chemical elemental demixing are shifted toward the endface of the torch along its symmetry axis for the regime II in comparison with the regime I. This correlates with the displacement of the embedded separation zones in the same direction for these cases. Fig. 7(b) demonstrates the distribution of the carbon element concentration and it elemental demixing.

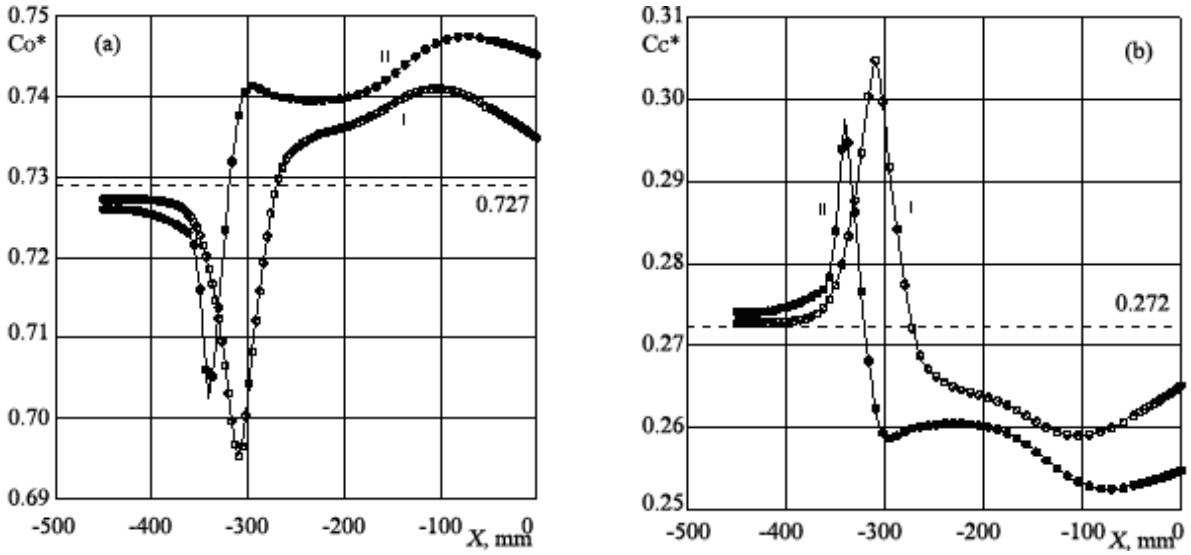

Figure 7: Distribution of the oxygen (a) and carbon (b) element concentrations along the symmetry axis of the torch for regimes I and II

Fig.8. represents the distributions of the non-charged components of the dissociated CO_2 flow and those of oxygen and carbon elements along the symmetry axis of the flow for regime I. In the vicinity of the stagnation point S_1 the mass concentrations of the atomic oxygen O and CO increase, while that fraction of the molecule CO_2 decreases. Intensive diffusion of the oxygen atoms from this region leads to the decrease of the oxygen element and increase of carbon one.

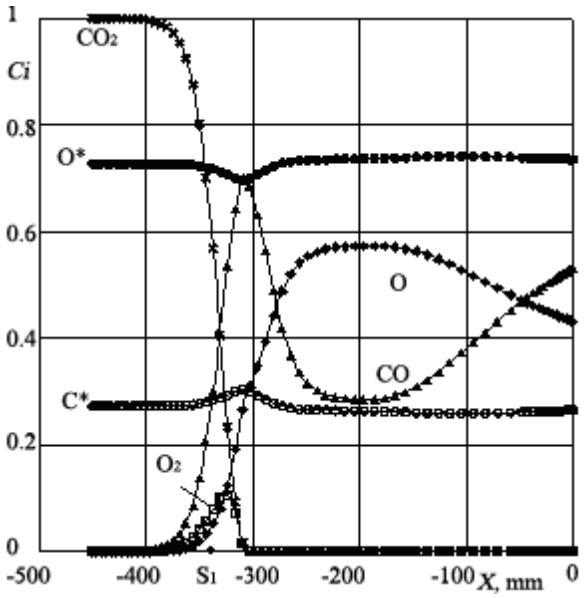

Figure 8: Distribution of oxygen and carbon element concentrations of the CO_2 mixture along the symmetry axis of the torch for regime I

Summary

The chemical elemental demixing was discovered during the numerical simulation of the inductive air and CO_2 plasma flows in the torch of IPG-4 plasmatron. The demixing mentioned is due to the difference in the rates of chemical dissociation-recombination reactions and to the difference of diffusion rates for the atomic and molecular components of the mixture.

The demixing effect is observable in the regions of the internal stagnation points, near the symmetry axis and the wall of the torch downstream. The oxygen element accumulation near the symmetry axis of the torch leads to higher concentration of this element in the flow exhaust from the torch into the low-pressure chamber with the experimental body in it. Such flow regime may cause intensified oxidation of the body surface. This effect must be taken into account in designing experimental studies on heat transfer modelling in inductive plasmatrons under hypersonic flight conditions.

The study was supported by the Russian Foundation for Basic Research (project № 11-01-00111) and by the basic research Program of Presidium RAS (project 25).

References

[1] Anfimov, N.A. 1963. Certain effects connected with multicomponent nature of gas mixtures. *Izv. Akad. Nauk SSSR. Mech. Mash.* 5:117–123.

[2] Tirskii, G.A. 1964. Determining effective diffusion coefficients in a laminar multicomponent boundary layer. *Dokl. Akad. Nauk SSSR.*. 155(6):1278–1281.

[3] Anfimov, N.A. 1964. Diffusive separation in a gas mixture in the presence of dissociation. *Dokl. Akad. Nauk SSSR.*. 156(6):1316–1319.

[4] Anfimov, N.A. 1964. Representation of dissociated air as a binary gas mixture in solving boundary layer problems. *Zh. Prikl. Mech. Tekhn. Fiz.* 1:47-52.

[5] Hirschfelder, J.O., Curtiss, C.F. and Bird, R.B. 1954. Molecular theory of gases and liquids. Wiley. New York.

[6] Gromov, V.G. 1966. Chemically nonequilibrium laminar boundary layer in dissociated air. *Fluid Dynamics*. 1(2):3-9.

[7] Kovalev, V.L. and Suslov, O.N. 1988. Diffusion separation of chemical elements on a catalytic surface. *Fluid Dynamics*. 23(4):579-585.

[8] Vasil'evskii, S.A. and Tirskii, G.A. 1994. Diffusion of elements and its influence on heat transfer in chemically equilibrium flows of multicomponent gases. In *Topical Gasdynamic and Physico-Chemical Models in Hypersonic Aerodynamics*. Part I [in Russian]:138-176.

[9] Rini, P., Vaden Abelee, D. and Degres, G. 2006. Elemental demixing in inductively coupled air plasma torches at high pressures. *J. Thermophys. Heat Transfer*. 20(1):31-40.

[10] Panesi, M., Rini, P., Degres, G. and Chazot, O. 2007. Analysis of chemical nonequilibrium and elemental demixing in plasmatron facility. *J. Thermophys. Heat Transfer*. 21(1):57-66.

[11] Kolesnikov, A.F. and Vasil'evskii, S.A. 1998. Results and problems of inductively coupled plasma flows modeling. Preprint N610. Institute for Problems in Mechanics, Russian Academy of Sciences, Moscow.

[12] Vasil'evskii, S.A. and Kolesnikov, A.F. 2000. Numerical simulation of equilibrium induction plasma flows in a cylindrical plasmatron channel. *Fluid Dynamics*. 35(5):769-777.

[13] Afonina, N.E., Gromov, V.G. and Sakharov, V.I. 2005. HIGHTEMP technique for high temperature gas flows numerical simulations. In: *5th Europ. Symp. 'Aerothermodynamics Space Vehicles'*. SP 563:323–328.

[14] Utyuzhnikov, S.V., Konyukhov, A.V. Rudenko, D.V., Vasil'evskii, S.A., Kolesnikov, A.F. and Chazot, O. 2004. Simulation of subsonic and supersonic flows in inductive plasmatrons. *AIAA J*. 42(9):1871-1877.

[15] Afonina, N.E., Vasil'evskii, S.A., Gromov, V.G., Kolesnikov, A.F., Pershin, I.S., Sakharov, V.I. and Yakushin, M.I. 2002. Flow and heat transfer in underexpanded air jets issuing from the sonic nozzle of a plasma generator. *Fluid Dynamics*. 37(5):803-813.

[16] Sakharov, V.I. 2007. Numerical simulation of thermally and chemically nonequilibrium flows and heat trasfer in underexpanded induction plasma jets. *Fluid Dynamics*. 42(6):1007-1015.

[17] Handbook of thermodynamic properties of individual matters. 1978. 1. (Books 1&2) [in Russian]. Nauka. Moscow.

[18] Godunov, S.K., Zabrodin, A.V., Ivanov, M. Ya., Kraiko, A.N. and Prokopov, G.P. 1976. Numerical solution of multidimensional problems of gasdynamics. [in Russian]. Nauka. Moscow.

[19] Ibragimova, L.V., Smekhov, G.D. and Shatalov, O.P. 1999.Dissociation rate constants of diatomic molecules under thermal equilibrium conditions. *Fluid Dynamics*. 34(1):153-157.

[20] Losev, S.A., Makarov, V.N. and Pogosbekyan, M. Yu. 1995. Model of the physico-chemical kinetics behind the front of a very intense shock wave in air. *Fluid Dynamics*. 30(2):299-310.

[21] Park, C. 1993. Review of chemical-kinetic problems of future NASA missions. Earth entries. *J. Thermophys. Heat Transfer*. 7(3):385-398.
[22] Park C., Howe J.T., Jaffe R.L. and Candler G.V. 1994. Review of chemical-kinetic problems of future NASA missons, II: Mars entries. *J.of Thermophys. Heat Transfer.* .7(3): 385–398.
[23] Ibragimova, L.V. 2000. Constants of chemical reactions rates in high temperature CO_2 gas. *Matemat. Modelirovanie.* 12(9):3–19.
[24] Losev, S.A., Makarov, V.N., Pogosbekyan, M. Yu., Shatalov, O.P. and Nikol'sky, V.S. 1990. Thermochemical nonequilibrium kinetic models in strong shock waves in air. *AIAA Paper N 94.*
[25] Ibraguimova, L.V., Smekhov, G.D., Shatalov, O.P., Eremin, A.V. and Shumova, V.V. 2000. Dissociation of CO_2 molecules in a wide temperature range. *High Temperature*. 38(1):37–40.
[26] Gupta, R.N. and Lee, K.P. 1994. An aerothermal study of MESUR pathfinder Aeroshell. *AIAA Paper N* 2025.
[27] Reid, R.C., Prausnitz, J.M. and Sherwood. 1977. The properties of gases and liquids. McCraw-Hill, New York.
[28] Afonina, N.E. and Gromov, V.G. 1998. Thermochemical nonequilibrium computations for a MARS express probe. In: *3rd Europ. Symp. 'Aerothermodynamics Space Vehicles'* ESTEC, Noordwijk:179–186.
[29] Gordeev, O.A., Kalinin, A.P., Komov, A.L., Lyusternik, V.E. and Samuilov, E.V. 1985. Reviews on thermopysical properties of matters [in Russian]. Inst. of High Temperatures. USSR Academy of Sciences. Moscow: 1-100.